Scattering from internal interfaces in microemulsion and sponge phases

G. Gompper and M. Schick*
Sektion Physik der Ludwig-Maximilians-Universität München, Theresienstrasse 37, 80333 München, Germany
(Received 31 August 1993)

The scattering intensity due to thermal fluctuations of the amphiphile density in microemulsion and sponge phases is calculated for a Ginzburg-Landau model with two scalar order parameters. The amphiphile correlations are found to be strongly influenced by the oil-water correlation function in the former and the water-water correlation function in the latter. We take these correlations to oscillate with wave vector k. Not only does this reproduce the known $1/q$ dependence of the scattering intensity for the small wave vector q, it also gives rise at $q = 2k$ to an experimentally observed peak. The calculated scattering intensities agree very well with experimental results over the whole range of wave vectors.

PACS number(s): 61.20.Gy, 05.40.+j, 82.70.−y

Two isotropic, homogeneous phases with a complex internal structure have been observed in amphiphilic systems [1]. One is the microemulsion, a bicontinuous mixture of oil, water, and amphiphile, found at low amphiphile concentrations, intermediate between that of the lamellar phase and of the coexisting water- and oil-rich phases. The other is the L_3, or sponge phase, observed in systems of water and amphiphile, at low amphiphile concentrations, intermediate between that of the lamellar phase and of the water-rich phase. The structure of these phases has been studied experimentally by both freeze-fracture microscopy [2,3] and neutron scattering [4,5]. From these experiments, the following picture emerges of the structure characterizing these phases. The microemulsion consists of coherent regions of oil and water, which are separated by an amphiphilic monolayer. The sponge phase has a similar structure, but the amphiphilic monolayer is replaced by a bilayer which separates two regions of water. In microemulsions, this structure leads to a scattering peak at finite wave vector in *bulk contrast* (i.e., when the scattering contrast is chosen between oil and water). This characteristic peak has been reproduced by several theoretical models, and can be traced to the structure of the fluid induced by the presence of the amphiphile, a structure described by an oscillatory water-water correlation function [4,5].

Scattering from the amphiphile film itself (*film contrast*) is found to be quite similar in the microemulsion and sponge phases [6]. It is a particularly important signal in the latter phase because there is no bulk contrast scattering due to the fact that the regions of water on either side of the bilayer are chemically identical. The signal typically consists of two peaks; the larger one at wave vector $q = 0$, and a much smaller one at a nonzero q. In the microemulsion, this value of q is twice the characteristic wave vector k of the bulk contrast scattering. This reflects the location of the amphiphile at the interfaces between oil and water and that there are two such interfaces in each period of the bulk fluid. In spite of the importance of the film contrast scattering in the sponge phase, it has not received a completely satisfactory theoretical explanation. Roux *et al.* [7] argued that a successful calculation of the film contrast signal would require that the coupling of the amphiphile bilayer to the two regions on either side of it be included, because the location of the bilayer was so intimately tied to these water regions. Therefore they employed a Ginzburg-Landau theory with two scalar order parameters; $\rho(\mathbf{r})$ representing the local deviation of the amphiphile concentration from its average value $\overline{\rho}$, and $\Phi(\mathbf{r})$, the difference in concentrations of the two regions of water. In their theory, the fluctuations of the water regions produce a water-water correlation with a *monotonic* exponential decay. Although not directly observable, these fluctuations couple to those of the amphiphile and produce a scattering intensity from the bilayer which peaks at $q = 0$, and decays as $1/q$ for small wave vector q. This is in good agreement with experimental observations [7–9]. However, their theory yields a film scattering intensity which decreases monotonically with q, and therefore fails to reproduce the smaller second peak whose presence is a very direct indication of the fluid structure.

We assume that the reason for this failure is that, in the description of Roux *et al.*, the sponge phase is not sufficiently structured, as evidenced by the monotonically decreasing water-water correlation function which they calculate. In the microemulsion, where one can observe the bulk contrast scattering which is related to the Fourier transform of this function, we know that the correlation function oscillates. Therefore we will generalize the model of Refs. [7,9] to allow for an oscillating correlation function, and use this model to calculate the scattering intensity in film contrast for both microemulsion and sponge phases. In doing so, we find not only the same good fit at small wave vectors to a $1/q$ decay obtained previously, but also a great improvement at larger q, including the description of the small peak at the appropriate wave vector. For sufficiently large q, we find that the scattering decays as $1/q^2$ as is observed experimentally [6].

*Permanent address: Department of Physics FM-15, University of Washington, Seattle, WA 98195.

Our analysis is based on the free-energy functional

$$\mathcal{F}\{\Phi,\rho\} = \mathcal{F}_0\{\Phi\} + \mathcal{F}_1\{\rho\} + \mathcal{F}_{\rm int}\{\Phi,\rho\}, \tag{1}$$

where

$$\mathcal{F}_0\{\Phi\} = \int d^3r \left[c(\nabla^2\Phi)^2 + g_0(\nabla\Phi)^2 + g_2\Phi^2(\nabla\Phi)^2 + \omega_2\Phi^2 + \omega_4\Phi^4 + \omega_6\Phi^6 \right], \tag{2}$$

$$\mathcal{F}_1\{\rho\} = \int d^3r \ \left[\alpha(\nabla\rho)^2 + \beta\rho^2\right], \tag{3}$$

and

$$\mathcal{F}_{\rm int}\{\Phi,\rho\} = \int d^3r \ \left[\tilde\gamma_1\rho\Phi^2 + \tilde\gamma_2(\nabla^2\rho)\Phi^2 + \tilde\gamma_3\rho\Phi(\nabla^2\Phi)\right] \tag{4}$$

for the two scalar order parameter fields $\Phi(\mathbf{r})$ and $\rho(\mathbf{r})$. In the microemulsion case, Φ is identified with the local concentration difference between oil and water, while in the case of the sponge phase Φ distinguishes water on one side ("inside") from water on the other side ("outside") of the amphiphilic bilayer. In both cases, ρ is the difference of local amphiphile concentration from the average amphiphile concentration $\bar\rho$, so that $\langle\rho\rangle = 0$. We have included in (4) all independent terms which are linear in ρ, quadratic in Φ, and contain no more than two derivatives [10,11]. Interpretation of these interactions is facilitated by integrating the second term by parts twice so that the free energy of interaction between the two order parameters becomes

$$\mathcal{F}_{\rm int}\{\Phi,\rho\} = \int d^3r \ \rho\left[\tilde\gamma_1\Phi^2 + (2\tilde\gamma_2+\tilde\gamma_3)\Phi\nabla^2\Phi + 2\tilde\gamma_2(\nabla\Phi)^2\right]. \tag{5}$$

In this form it is seen that the three combinations Φ^2, $\Phi\nabla^2\Phi$, and $(\nabla\Phi)^2$ all act as chemical potentials for the amphiphile. Provided that $\tilde\gamma_2 < 0$, the third term favors larger than average amphiphile concentrations at an interface. If $\tilde\gamma_1 > 0$, the first term favors smaller than average amphiphile concentrations in the bulk phases. Similarly, if $2\tilde\gamma_2 + \tilde\gamma_3 < 0$, the second term favors smaller than average amphiphile concentrations on both sides of a planar interface. For curved interfaces, the role of this term is more complex because $\nabla^2\Phi$ contains contributions proportional to the mean curvature of the interface.

The average concentration of amphiphile, $\bar\rho$, enters the model via the parameters g_0 and ω_2. For small amphiphile concentrations, g_0 is large and positive. With increasing $\bar\rho$, g_0 decreases and eventually becomes negative. Were the density ρ in the above two-component Landau theory integrated out, and the expression remaining expanded in powers of Φ and its gradients, the result would be a one-component Landau theory of the form which has been much used in the study of amphiphilic systems [12].

In order to obtain the scattering intensity in film contrast, we must calculate the structure function

$$G_{\rho\rho}(q) = \langle\rho(\mathbf{q})\rho(-\mathbf{q})\rangle. \tag{6}$$

In the absence of interaction between the two order parameter fields, (i.e., for $\tilde\gamma_1 = \tilde\gamma_2 = \tilde\gamma_3 = 0$), this function is easily calculated in the Ornstein-Zernike approximation and reads

$$G^{(0)}_{\rho\rho}(q) \equiv \langle\rho(\mathbf{q})\rho(-\mathbf{q})\rangle_1 = \frac{1}{2}\frac{\alpha^{-1}}{q^2+\xi_\rho^{-2}}, \tag{7}$$

where $\langle\rangle_1$ denotes the averages with a free-energy functional (3), and $\xi_\rho^{-2} = \beta/\alpha$ is the correlation length of the ρ fluctuations. Similarly, the structure function

$$G_{\Phi\Phi}(q) \equiv \langle\Phi(\mathbf{q})\Phi(-\mathbf{q})\rangle \tag{8}$$

in the same approximation is

$$G^{(0)}_{\Phi\Phi}(q) \equiv \langle\Phi(\mathbf{q})\Phi(-\mathbf{q})\rangle_0 = \frac{1}{2}\frac{1}{cq^4+g_0q^2+\omega_2}, \tag{9}$$

where $\langle\rangle_0$ denotes the averages with a free-energy functional (2), with $g_2 = 0$ and $\omega_4 = \omega_6 = 0$. Its Fourier transform, which is the correlation function in this approximation, is [4]

$$G^{(0)}_{\Phi\Phi}(r) \equiv \langle\Phi(\mathbf{r})\Phi(0)\rangle_0 = \frac{A}{r}e^{-r/\xi}\sin(kr), \tag{10}$$

where

$$\xi^{-2} = \frac{1}{2}\sqrt{\frac{\omega_2}{c}} + \frac{1}{4}\frac{g_0}{c}, \quad k^2 = \frac{1}{2}\sqrt{\frac{\omega_2}{c}} - \frac{1}{4}\frac{g_0}{c},$$
$$A = \frac{\xi}{16\pi ck}. \tag{11}$$

The above form which displays the nonmonotic oscillatory behavior characteristic of the complex fluid is valid for $g_0^2 < 4c\omega_2$. The wave vector k characterizes the oscillations in the concentration of oil in the microemulsion, or of one of the two regions of water in the sponge phase. In contrast, Refs. [7,9] assume that $c = 0$ and g_0 is positive, in which case $G^{(0)}_{\Phi\Phi}$ decays monotonically.

The effect of the fluctuations of the order parameter $\Phi(\mathbf{r})$ on $G_{\rho\rho}$ can be calculated in an expansion in the interaction $\mathcal{F}_{\rm int}$. This leads to a series of Feynman diagrams with three different vertices and two different propagators. To lowest order in the coupling constants $\tilde\gamma_1$, $\tilde\gamma_2$, and $\tilde\gamma_3$, we obtain the diagrams shown in Fig. 1. Details of the calculation of these diagrams are given in the Ap-

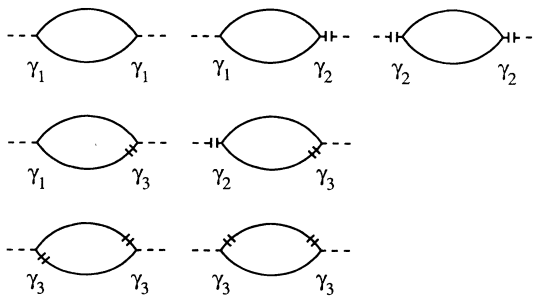

FIG. 1. The seven different Feynman diagrams, which contribute to the correlation function $\langle\rho(\mathbf{k})\rho(-\mathbf{k})\rangle$ to lowest nontrivial order in the coupling constants $\tilde\gamma_1$, $\tilde\gamma_2$, and $\tilde\gamma_3$. Here, a full line denotes the bare propagator $G^{(0)}_{\Phi\Phi}$, a dashed line the bare propagator $G^{(0)}_{\rho\rho}$. Bars at the end of a line denote derivatives.

pendix. The result of the calculation to second order in the couplings can be written

$$G_{\rho\rho}(q) = G^{(0)}_{\rho\rho}(q) + G^{(0)}_{\rho\rho}(q)\Gamma(q\xi, k\xi)G^{(0)}_{\rho\rho}(q), \tag{12}$$

where

$$\frac{\xi_\rho^2}{2\alpha}\Gamma(x,y) = (\gamma_1 - \gamma_2 x^2)^2\Lambda_-(x,y) + 2\gamma_3(\gamma_1 - \gamma_2 x^2)\left[(1-y^2)\Lambda_-(x,y) - y\Xi(x,y)\right] + \gamma_3^2\left\{2y^2\left[\Lambda_+(x,y) - \Lambda_-(x,y)\right] + (1-y^2)^2\Lambda_-(x,y) - 2y(1-y^2)\Xi(x,y) + y^2\right\} \tag{13}$$

with

$$\Lambda_\pm(x,y) = \frac{1}{4x}\left[2\arctan\left(\frac{x}{2}\right) \pm \arctan\left(\frac{4x}{4+4y^2-x^2}\right) \pm n\pi\right], \tag{14}$$

$$\Xi(x,y) = \frac{1}{4x}\ln\left(\frac{4+(x+2y)^2}{4+(x-2y)^2}\right). \tag{15}$$

Here, $n = 0$ for $0 \le x^2 < 4+4y^2$ and $n = 1$ for $x^2 > 4+4y^2$. The dimensionless coupling constants are $\gamma_1 = \tilde{\gamma}_1 A\xi_\rho\sqrt{(4\pi\xi)/\alpha}$, $\gamma_2 = \tilde{\gamma}_2 A\xi^{-2}\xi_\rho\sqrt{(4\pi\xi)/\alpha}$, and $\gamma_3 = \tilde{\gamma}_3 A\xi^{-2}\xi_\rho\sqrt{(4\pi\xi)/\alpha}$.

The asymptotic behavior of a typical vertex function $\Gamma(q\xi, k\xi)$ for $1 \ll k\xi$ and either $q\xi \ll k\xi$ or $q\xi \gg k\xi$ can be derived straightforwardly from Eq.(13). For $q\xi \ll k\xi$,

$$\frac{\xi_\rho^2}{2\alpha}\Gamma(q\xi, k\xi) = \frac{1}{2}\gamma_3^2(q\xi)^{-1}\arctan\left(\frac{q\xi}{2}\right)(k\xi)^4 + \left[\frac{7}{4}\gamma_3^2 - \gamma_3\left(\gamma_1 + \gamma_3 - \gamma_2(q\xi)^2\right)(q\xi)^{-1} \times \arctan\left(\frac{q\xi}{2}\right)\right](k\xi)^2 + O(k\xi). \tag{16}$$

A numerical comparison of this result with Eq. (13) shows that $\Gamma(q\xi, k\xi)$ is described very well by Eq. (16) for $q\xi \le k\xi$. Note that for $q\xi$ much less than unity, $\Gamma(q\xi, k\xi)$ is almost constant at its peak $q = 0$ value, while for $q\xi$ of order unity or greater, it decreases as $1/q$. For small q, $G^{(0)}_{\rho\rho}(q)$ is constant, so that the behavior of the scattering intensity $G_{\rho\rho}$ is, from Eq. (12), a decrease like $1/q$.

In the opposite limit, $q\xi \gg k\xi \gg 1$,

$$\frac{\xi_\rho^2}{2\alpha}\Gamma(q\xi, k\xi) = (2\gamma_2 + \gamma_3)^2(k\xi)^2 + \pi\gamma_3^2(k\xi)^2\,(q\xi)^{-1} + \frac{4}{3}[-6\gamma_1\gamma_2 - 24\gamma_2^2 - 3\gamma_1\gamma_3 - 18\gamma_2\gamma_3 - 6\gamma_3^2 + (12\gamma_2^2 + 10\gamma_2\gamma_3 + 3\gamma_3^2)(k\xi)^2] \times (k\xi)^2\,(q\xi)^{-2} + O((q\xi)^{-3}). \tag{17}$$

A numerical comparison of this result with Eq. (13) shows that $\Gamma(q\xi, k\xi)$ is described very well by Eq. (17) for $q\xi \ge 3k\xi$. As $\Gamma(q\xi, k\xi)$ approaches a constant in this limit, and $G^{(0)}_{\rho\rho}(q)$ falls as $1/q^2$, we see from the first term of Eq. (12) that the film scattering also falls as $1/q^2$. This is in agreement with experiment, but does not arise from the structure of the film as in the interpretation of Ref. [6], but rather from the bulk density of amphiphile.

Two selected scattering intensities are shown in Figs. 2 and 3. In Fig. 2, the parameters are chosen such as to make the scattering intensity show all essential features observed in neutron scattering experiments on the *ternary* system D_2O–C_8D_{18}–*n*-alkyl polyglycol ether (C_8E_3), measured in film contrast by Schubert and Strey [13]. In Fig. 3, a different choice yields a scattering intensity which agrees quantitatively with that observed in the quasibinary system Aerosol OT (AOT)–brine, as given by Skouri *et al.* [14]. The agreement with the experiments could be improved further by attempting to fit the data. It would be very interesting to examine the bulk and film scattering from the same microemulsion using for the bulk contrast the Teubner-Strey form, Eq. (9) and for the film contrast our Eqs. (12) and (13). The bulk contrast would yield the values of ξ and k needed for the film contrast. A good fit would confirm that the clear physical connection between the amphiphiles and the bulk regions they divide causes the bulk and film scattering to be intimately related.

We wish to thank J. Goos and H. Wagner for helpful discussions. M.S. is grateful to Herbert Wagner for his hospitality at the Ludwig-Maximilians Universität München, and to the Alexander von Humboldt-Stiftung for financial support. This work was supported in part by the Deutsche Forschungsgemeinschaft through Sonderforschungsbereich 266, and by the National Science Foundation under Grant No. DMR9220733.

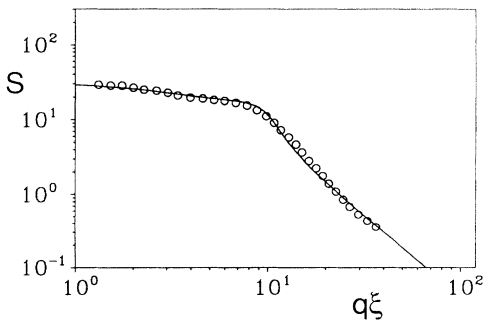

FIG. 2. Amphiphile-amphiphile scattering intensity S (unnormalized) in the microemulsion phase of the ternary system D_2O-C_8D_{18}-C_8E_3. The full line is the theoretical result for the dimensionless quantity $(\alpha/\xi_\rho^2)G_{\rho\rho}$ calculated with parameters $\xi_\rho/\xi = 0.05$, $k\xi = 5.0$, $\gamma_1 = 8.0$, $\gamma_2 = -0.10$, and $\gamma_3 = -0.12$. Data points are taken from Ref. [13]. The experimental correlation length is assumed to be $\xi \simeq 100$ Å.

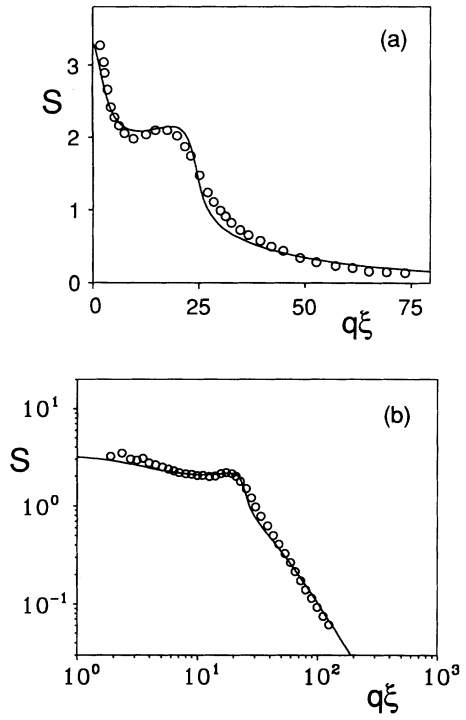

FIG. 3. Amphiphile-amphiphile scattering intensity S (unnormalized) in the L_3 phase of the system (AOT)-brine. The full line is the theoretical result for the dimensionless quantity $(\alpha/\xi_\rho^2)G_{\rho\rho}$ calculated with parameters $\xi_\rho/\xi = 0.03$, $k\xi = 12.0$, $\gamma_1 = 0.0$, $\gamma_2 = -0.014$, and $\gamma_3 = -0.021$. Data points are taken from Ref. [14] for amphiphile volume fraction $\bar{\rho} = 0.0675$. (a) Linear axes. (b) Double-logarithmic plot. The $1/q^2$ behavior for $q > 2k$ is clearly visible. The experimental correlation length is assumed to be $\xi \simeq 1350$ Å.

APPENDIX: FEYNMAN DIAGRAMS

Four different integrals have to be evaluated in order to calculate the various Feynman diagrams:

$$\begin{aligned} I_1(q) &= \int d^3r\ e^{i\mathbf{q}\cdot\mathbf{r}}\ \left[G^{(0)}_{\Phi\Phi}(r)\right]^2, \\ I_2(q) &= \int d^3r\ e^{i\mathbf{q}\cdot\mathbf{r}}\ G^{(0)}_{\Phi\Phi}(r)\nabla^2 G^{(0)}_{\Phi\Phi}(r), \\ I_3(q) &= \int d^3r\ e^{i\mathbf{q}\cdot\mathbf{r}}\ \left[\nabla^2 G^{(0)}_{\Phi\Phi}(r)\right]^2, \\ I_4(q) &= \int d^3r\ e^{i\mathbf{q}\cdot\mathbf{r}}\ G^{(0)}_{\Phi\Phi}(r)\nabla^2\nabla^2 G^{(0)}_{\Phi\Phi}(r). \end{aligned} \tag{A1}$$

With the correlation function $G^{(0)}_{\Phi\Phi}(r)$, Eq. (10), we easily obtain

$$\begin{aligned} \nabla^2 G^{(0)}_{\Phi\Phi}(r) &= \frac{\partial^2}{\partial r^2} G^{(0)}_{\Phi\Phi}(r) + \frac{2}{r}\frac{\partial}{\partial r} G^{(0)}_{\Phi\Phi}(r) \\ &= \frac{A}{r\xi^2} e^{-r/\xi}\Big\{ \left[1-(k\xi)^2\right]\sin(kr) \\ &\qquad -2k\xi\cos(kr)\Big\} \end{aligned} \tag{A2}$$

and similarly

$$\begin{aligned} \nabla^2\nabla^2 G^{(0)}_{\Phi\Phi}(r) = \frac{A}{r\xi^4} e^{-r/\xi}\Big(&\Big\{\left[1-(k\xi)^2\right]^2 - 4(k\xi)^2\Big\} \\ &\times \sin(kr) - 4k\xi\left(1-(k\xi)^2\right)\cos(kr)\Big) \\ &+4\pi A\frac{2k}{\xi}\delta(\mathbf{r}). \end{aligned} \tag{A3}$$

The evaluation of the integrals (A1) is then straightforward, and yields

$$I_1(q) = 4\pi A^2\xi\Lambda_-(q\xi, k\xi), \tag{A4}$$

$$\begin{aligned} I_2(q) = 4\pi A^2\xi^{-1}\Big\{ &\left(1-(k\xi)^2\right)\Lambda_-(q\xi,k\xi) \\ &-k\xi\Xi(q\xi,k\xi)\Big\}, \end{aligned} \tag{A5}$$

$$\begin{aligned} I_3(q) = 4\pi A^2\xi^{-3}\{ &+4(k\xi)^2\Lambda_+(q\xi,k\xi) \\ &+\left[1-(k\xi)^2\right]^2\Lambda_-(q\xi,k\xi) \\ &-2k\xi\left[1-(k\xi)^2\right]\Xi(q\xi,k\xi)\}, \end{aligned} \tag{A6}$$

$$\begin{aligned} I_4(q) = 4\pi A^2\xi^{-3}\{ &-4(k\xi)^2\Lambda_-(q\xi,k\xi) \\ &+[1-(k\xi)^2]^2\Lambda_-(q\xi,k\xi) \\ &-2k\xi[1-(k\xi)^2]\Xi(q\xi,k\xi)+2(k\xi)^2\}, \end{aligned} \tag{A7}$$

where the functions $\Lambda_\pm(q\xi, k\xi)$ and $\Xi(q\xi, k\xi)$ have been defined in Eqs. (14) and (15).

To illustrate the calculation of the Feynman diagrams shown in Fig. 1, we want to give here some details of the calculation of one of the diagrams with two γ_3 vertices. In position space, it is

$$\begin{aligned} F_{33}(\mathbf{r}_1,\mathbf{r}_2) = \tilde{\gamma}_3^2 \int d^3r_1' \int d^3r_2' G^{(0)}_{\rho\rho}(\mathbf{r}_1-\mathbf{r}_1') \\ \times\nabla^2_{\mathbf{r}_1'} G^{(0)}_{\Phi\Phi}(\mathbf{r}_1'-\mathbf{r}_2')\nabla^2_{\mathbf{r}_2'} G^{(0)}_{\Phi\Phi}(\mathbf{r}_1'-\mathbf{r}_2') \\ \times G^{(0)}_{\rho\rho}(\mathbf{r}_2'-\mathbf{r}_2). \end{aligned} \tag{A8}$$

In Fourier space, the same contribution reads

$$F_{33}(q) = \tilde{\gamma}_3^2 G^{(0)}_{\rho\rho}(\mathbf{q}) \int d^3r\ e^{i\mathbf{q}\cdot\mathbf{r}} \left[\nabla^2_{\mathbf{r}} G^{(0)}_{\Phi\Phi}(\mathbf{r})\right]^2 G^{(0)}_{\rho\rho}(\mathbf{q}), \tag{A9}$$

where $\mathbf{r} = \mathbf{r}_1' - \mathbf{r}_2'$. Thus

$$F_{33}(q) = \tilde{\gamma}_3^2 G^{(0)}_{\rho\rho}(\mathbf{q})^2\ I_3(q), \tag{A10}$$

where $I_3(q)$ has been calculated above. The other Feynman diagrams can be calculated along the same lines.

[1] *Physics of Amphiphilic Layers*, edited by J. Meunier, D. Langevin, and N. Boccara, Springer Proceedings in Physics Vol. 21 (Springer, Berlin, 1987); *The Structure and Conformation of Amphiphilic Membranes*, edited by R. Lipowsky, D. Richter, and K. Kremer (Springer, Berlin, 1992); G. Gompper and M. Schick, in *Phase Transitions and Critical Phenomena*, edited by C. Domb and J. Lebowitz (Academic, London, in press).

[2] W. Jahn and R. Strey, J. Chem. Phys. **92**, 2294 (1988).

[3] R. Strey, W. Jahn, G. Porte, and P. Bassereau, Langmuir **6**, 1635 (1990).

[4] M. Teubner and R. Strey, J. Chem. Phys. **87**, 3195 (1987).

[5] C.G. Vonk, J.F. Billman, and E.W. Kaler, J. Chem. Phys. **88**, 3970 (1988).

[6] R. Strey, J. Winkler, and L. Magid, J. Phys. Chem. **95**, 7502 (1991).

[7] D. Roux, M.E. Cates, U. Olsson, R.C. Ball, F. Nallet, and A.M. Bellocq, Europhys. Lett. **11**, 229 (1990).

[8] C. Coulon, D. Roux, and A.M. Bellocq, Phys. Rev. Lett. **66**, 1709 (1991).

[9] D. Roux, C. Coulon, and M.E. Cates, J. Phys. Chem. **96**, 4174 (1992).

[10] All other terms with two derivatives, such as $\Phi(\nabla\rho\cdot\nabla\Phi)$, can be obtained by partial integrations. The term with coefficient $\tilde{\gamma}_3$ was not considered in Refs. [7,9].

[11] The terms of order Φ^4, Φ^6, and $\Phi^2(\nabla\Phi)^2$ with g_2 sufficiently large and positive have to be included in the model to ensure thermodynamic stability. They play no role in the calculation of the scattering intensity presented here.

[12] G. Gompper and M. Schick, Phys. Rev. Lett. **65**, 1116 (1990).

[13] K.-V. Schubert and R. Strey, J. Chem. Phys. **95**, 8532 (1991).

[14] M. Skouri, J. Marignan, J. Appell, and G. Porte, J. Phys. (Paris) II **1**, 1121 (1991).